



Accepted Article

Title: Intervalence Charge Transfer and Exothermic and Isoenergetic Symmetry Breaking Charge Separation in Far-Red Capturing Zinc Phthalocyanine Dimers

Authors: Ram R. Kaswan, Desiré Molina, Lydia Ferrer-López, Javier Ortiz, Paul A. Karr, Ángela Sastre-Santos, and Francis D'Souza

This manuscript has been accepted after peer review and appears as an Accepted Article online prior to editing, proofing, and formal publication of the final Version of Record (VoR). The VoR will be published online in Early View as soon as possible and may be different to this Accepted Article as a result of editing. Readers should obtain the VoR from the journal website shown below when it is published to ensure accuracy of information. The authors are responsible for the content of this Accepted Article.

To be cited as: Angew. Chem. Int. Ed. 2025, e202502516

Link to VoR: https://doi.org/10.1002/anie.202502516



Intervalence Charge Transfer and Exothermic and Isoenergetic Symmetry Breaking Charge Separation in Far-Red Capturing Zinc Phthalocyanine Dimers

Ram R. Kaswan, [a] Desiré Molina, [b] Lydia Ferrer-López, [b] Javier Ortiz, [b] Paul A. Karr, [c] Ángela Sastre-Santos*[b], and Francis D'Souza*[a]

[a] R. R. Kaswan, Prof. F. D'Souza

Department of Chemistry

University of North Texas

1155 Union Circle, 305070, Denton, TX 76203-5017, USA

E-mail: Francis.DSouza@unt.edu

[b] D. Molina, L. Ferrer-López, J. Ortiz, Prof. A. Sastre-Santos Área de Química Orgánica, Instituto de Bioingeniería Universidad Miguel Hernández Avda

de la Universidad s/n 03203 Elche, Spain

E-mail: asastre@umh

[c] Prof. P. A. Karr

Department of Physical Sciences and Mathematics

Wayne State College

1111 Main Street, Wayne, Nebraska 68787, USA

E-mail: pakarr1@wsc.edu

Supporting information for this article is given via a link at the end of the document.

Abstract: Orientation and distance-dependent intervalence charge transfer phenomenon is demonstrated in far-red capturing zinc phthalocyanine dimers connected by a bis-acetylene-phenyl π-spacer (ortho, meta, or para positions) upon oxidizing one of the phthalocyanine rings, resulting in split oxidation waves and a new optical transition in the near-infrared region. Optical studies initially probed the symmetry-breaking charge separation events in these dimers wherein solvent polarity-dependent quenching was witnessed. Interestingly, efficient quenching in nonpolar toluene was also seen for the ortho-dimer. Free-energy calculations supported symmetry-breaking charge separation in polar solvents and the ortho-dimer even in nonpolar solvents under isoenergetic (endothermic by ~40 mV) conditions. Molecular electrostatic potential maps generated on DFT-optimized structures revealed quadrupolar charge transfer states, more so in polar media. The time-dependent DFT calculations revealed the conversion of the quadrupolar charge transfer states to bipolar charge-separated states from different singlet-singlet excitations. Femtosecond transient absorption studies covering broad temporal and spatial scales provided evidence for the charge separation process, including that for the ortho-dimer in toluene, where an isoenergetic process was predicted. The charge-separated states lasted for 200-500 ps depending upon dimer linkage. These unprecedented findings reveal the potential applications of the investigated phthalocyanine dimers in energy harvesting, photocatalytic, and pertinent optoelectronic applications.

Introduction

Discoveries leading to new phenomena in molecular systems open new avenues for scientific and technological advances.^[1-3] This applies explicitly to electro- and photochemical events as

they are commonly employed in myriad applications, including energy harvesting, fuel production, energy storage, and catalyst development. The three-dimensional arrangement of π -conjugated organic molecular systems in photosynthesis is crucial as it ensures efficient solar energy harvesting, transport, and conversion. The striking solar photons are transferred into the reaction center in the photosynthetic systems through coherent exciton transport. The conversion of excitation energy to chemical energy at the reaction center is initiated by the symmetry-breaking charge separation process (SB-CS), which triggers the sequential electron transfer events leading to long-lived charge-separated states, which are eventually used in the conversion of adenine diphosphate (ADP) to adenine triphosphate (ATP). The comprehensive understanding of the photophysical events, viz., exciton formation, energy transfer, and charge separation, in synthetic molecular systems and their precise dependence on the spatial arrangement, π -overlap, and intermolecular distances is not just essential but a cornerstone for the design of efficient and robust artificial solar energy conversion systems.

Photoinduced SB-CS is a process where a symmetrical pair of identical chromophores forms a charge-separated state with the hole and electron on different chromophores, i.e., M-M + h $\nu \rightarrow M^+$ - M^- , upon photoexcitation with high efficiency.^[17,18] SB-CS has found wide applications in artificial photosynthesis and optoelectronic devices owing to the minimal energy loss during the charge-separated state formation (energy loss between the exciton and chargeseparated state is <100 mV for SB-CS, in contrast to the value of ~500 mV or more for charge separation in traditional donor-acceptor systems).^[19] SB-CS rate mainly depends on electronic coupling strength and solvent environment.[17-19] In a weak exciton coupling regime, the electronic absorption spectra of the interacting chromophores show minor variation compared to the noninteracting systems. Theoretically, the excited states of the molecular dimer can be represented as locally excited singlet (LE) states and charge-separated (CS) states. [20,21] A literature survey shows that SB-CS processes in weakly coupled dimers and trimers of perylene and pentacene, [29-31] BODIPY, [17,32,33] metallopyrrins, [31,34] perylenediimide.[21-28] subphthalocyanine, [36] and terrylenediimide [37-38] are well explored. In some bianthryl.[35] instances, efforts have been put into probing SB-CS processes in film samples, metal-organic frameworks, and polymers. [39-43] Unfortunately, almost all the reported systems used high-energy visible light (1.8 - 3.0 eV) to initiate SB-CS due to the limited optical coverage of these chromophore dimers (absorption mainly in the near-UV and visible spectral range). Unlike natural photosynthesis, photosystems I and II use far-red 680 and 700 nm light to initiate the SB-CS process. [44,45] This is also true for bacterial photosynthetic systems where near-infrared (near-IR) initiates the SB-CS process. For example, R. Sphaeroides uses near-IR light of 870 nm, and some bacteriochlorophyll species even use light up to 940 nm to initiate the SB-CS process. [46-^{47]} Thus, a critical knowledge gap exists due to the lack of synthetic molecular dimers capable of undergoing SB-CS with low-energy light excitation from the far-red and near-IR regions.

Intervalence (or charge resonance) compounds^[48-52] comprise two redox centers with different oxidation states connected by a bridge. These are model systems to study the fundamentals of electron transfer events and to develop the field of single-molecule electronics.^[53-55] Observed initially in inorganic bis-Ruthenium Creutz-Taube type complexes, organic systems are also known to exhibit such phenomena.^[48] Charge localization and delocalization are of importance in mixed-valence systems. For one-electron mixed valence compounds comprised of two redox sites connected by a bridge, two extreme cases, viz., Rⁿ⁺-bridge-R⁽ⁿ⁺¹⁾⁺ (complete localization), and R^{(n+0.5)+}-bridge-R^{(n+0.5)+} (full delocalization), and anything in between is possible. Per Robin and Day classification, ^[56-58] completely localized systems belong to class I, fully delocalized systems are class III, and systems in between belong to class II (partial delocalization). The classical theory predicts the class II type to exhibit a highly solvent-dependent Gaussian type intervalence charge transfer (IVCT) band in the near-infrared region

due to optically induced charge transfer from one redox center to the other. In contrast, the IVCT is asymmetrical (possibly with a vibrational fine structure) for the class III type) and largely solvent-independent. Such a phenomenon is observed in simple redox-active molecular dimers but not in large π -conjugated systems.

Phthalocyanines are a class of electro- and photoactive molecular systems nowadays commonly used in basic research and industrial applications due to their higher stability (e.g., coloring pigments for fabric and toners in color printing and xerography) and highly tunable physico-chemical properties, especially optical coverage with strong absorptivity well into the farred and near-IR regions.^[59,60] Consequently, discoveries in this class of molecules are expected to advance scientific understanding pertinent to many applications.^[61,62]

To address the above-narrated knowledge gap of lacking far-red and near-IR molecular systems revealing SB-CS with low-energy light excitation and that synthetic phthalocyanines fulfill such needs, in the present study, we have built zinc phthalocyanine dimers (ZnPc dimers) shown in Figure 1. The two ZnPc units are covalently attached to an acetylene π -linker with a central phenyl ring. The phenyl rings' ortho, meta, and para-positions have been used to build the dimers to visualize the distance and orientation effects. As demonstrated here, these dimers undergo the anticipated SB-CS under both exothermic and isoenergetic conditions. Additionally, they reveal the much-anticipated intervalence charge transfer (IVCT) when one of the two ZnPc units is oxidized. DFT and time-dependent DFT (TD-DFT) studies were able to pinpoint the exact excited states involved in the CB-CS process. This is the first example of ZnPc dimers showing IVCT and its significance in the SB-CS process. Key findings are summarized below.

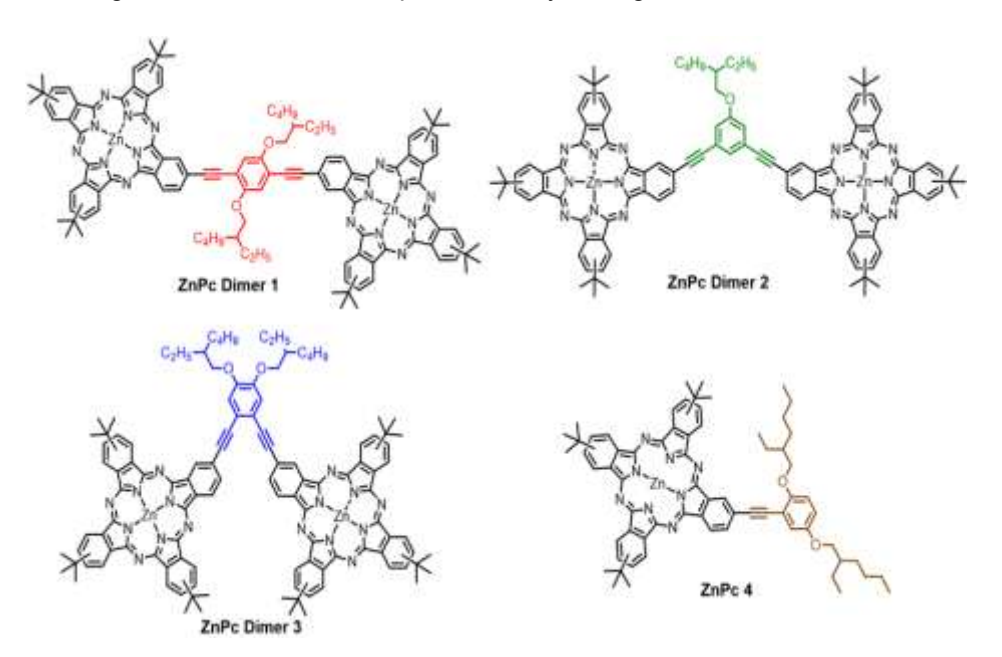
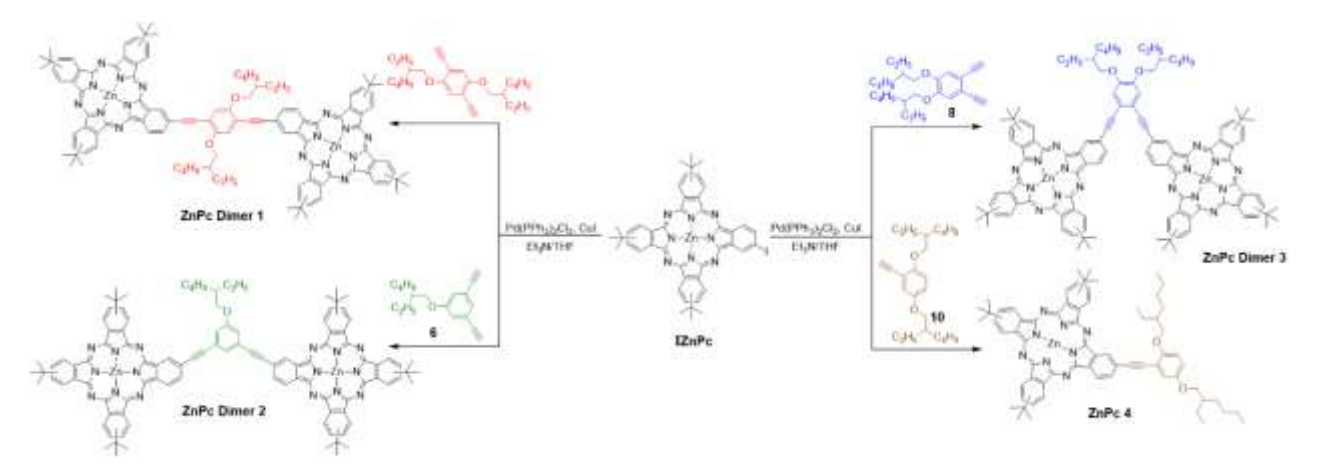


Figure 1. The structure of the ZnPc dimers and the ZnPc monomer investigated in the present study.

Optical studies

SB-CS in symmetric dimers occurs due to polar solvents' solvent stabilization of charge-separated states. A simple solution study of the emission behavior in nonpolar and polar solvents would provide the first indication of SB-CS in the dimers. Figure 2 shows the normalized to the visible band absorption and fluorescence spectra of the investigated compounds in nonpolar toluene (dielectric constant, $\varepsilon = 2.38$) and polar benzonitrile (PhCN, $\varepsilon = 26$), while relevant data are summarized in Table 1. Only in the case of the *ortho* dimer, **3**, the visible band revealed a blue

shift of 10-12 nm, while the other two dimers revealed a small redshift. The ratio of the $A_{0,0}/A_{0,1}$ peak intensity was higher for the *ortho* dimer than the other two dimers, and the monomer suggested strong intramolecular interactions in the *ortho* dimer irrespective of the solvent media.^[18]



Scheme 1. ZnPc dimers 1, 2, and 3, and ZnPc monomer, 4.

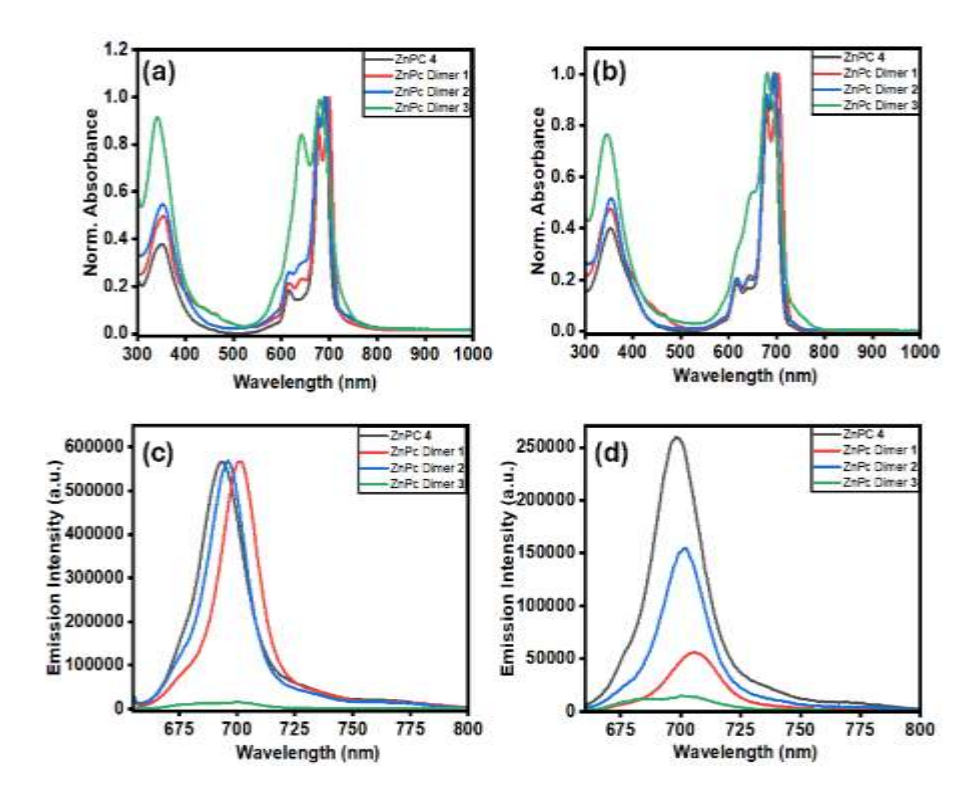


Figure 2. Absorption (a and b) and fluorescence (c and d) of the indicated compounds in toluene (a and c) and benzonitrile (b and d). The compounds were excited at 650 nm, keeping the optical density visible band at 0.1.

Table 1. Spectroscopic properties of the investigated compounds in nonpolar and polar solvents to help establish the occurrence of SB-CS.

	Toluene				PhCN			
	4	3	2	1	4	3	2	1
$\lambda_{abs}(A_{0-0})$, nm	690	680	693	699	693	681	696	704
$\lambda_{abs}(A_{0-1})$, nm	679	643	677	677	680	650	679	679
$\hat{\lambda_{em}}$, \hat{nm}	694	700	696	701	698	700	702	706
<i>E</i> _{0,0} eV	1.79	1.80	1.78	1.77	1.78	1.80	1.77	1.76
A_{0-0}/A_{0-1}	1.12	1.16	1.06	1.12	1.12	1.73	1.08	1.15
$\Delta \tilde{v}$ Stokes ,cm ⁻¹	84	420	62	42	104	399	122	42
φ _{Fl} ^a , %	23	< 1	18	17	12	< 1	6	2
τ _{Fl} , ns	2.6	-	2.44	2.27	2.26	-	0.98	0.47
k_r , $10^7 \mathrm{s}^{-1}$	8.8	-	7.4	7.48	5.4	-	6	4.3
k_{nr} , $10^7 s^{-1}$	29	-	34	36	39	-	96	208

^a Photoluminescence intensity with respect to ZnPc monomer

The fluorescence spectrum of the dimers in toluene did not reveal appreciable guenching for the meta and para dimers, while significant quenching (>95%) was observed in toluene for the ortho dimer, 3. Interestingly, in benzonitrile, all three dimers revealed quenching compared to that of the monomer and followed the order: 1 (50%) < 2 (76%) < 3 (92%). Such was the case for fluorescence lifetimes determined from time-correlated single-photon counting techniques (TCSPC, see Figure S9 for decay profiles). While the lifetime for 3 was within the time resolution of our setup (~200 ps) in both solvents, reduced lifetimes for 1 and 2 were observed in benzonitrile (often a short-lived component representing SB-CS and a long-lived component representing regular fluorescence). The significant quenching observed here suggests the occurrence of excited state events in polar benzonitrile for all dimers and in nonpolar toluene in the case of 4. The calculated rates of radiative, k_r , and nonradiative, k_{nr} , are listed in Table 1. Higher k_{nr} was witnessed for the dimers compared to the monomer. Figure 3 shows the cyclic voltammograms (CVs) of the compounds investigated in DCB containing 0.1 M (TBA)CIO₄. The ZnPc monomer, 4 revealed a single one-electron reversible oxidation at $E_{1/2}$ = 0.65 V vs. Ag/AgCl. Multi-cycling did not change the shape or position of this redox wave. Compound 4 also revealed two oneelectron reversible reductions at $E_{1/2}$ = -0.94 and -1.27 V. In contrast, the first oxidation process of the dimers revealed a split wave, while the reductions retained their basic characteristics with a slight cathodic shift. In the case of ortho dimer, 3, the split oxidation peaks were located at 0.57 and 0.71 V, which is a 140-mV splitting.

In the case of *meta* dimer, **2**, the peaks were located at 0.57 and 0.70 V with a 130-mV split. In the case of *para* dimer, **1**, the splitting was too close with a 120-mV split. The splitting reveals the stepwise removal of electrons from the dimer according to Equation 1.^[63]

$$ZnPc-sp-ZnPc \stackrel{-e^-}{=} ZnPc^{-+}-sp-ZnPc \stackrel{-e^-}{=} ZnPc^{-+}-sp-ZnPc^{-+}$$

$$Charge Resonance$$

$$ZnPc-sp-ZnPc^{-+}$$

$$ZnPc-sp-ZnPc^{-+}$$

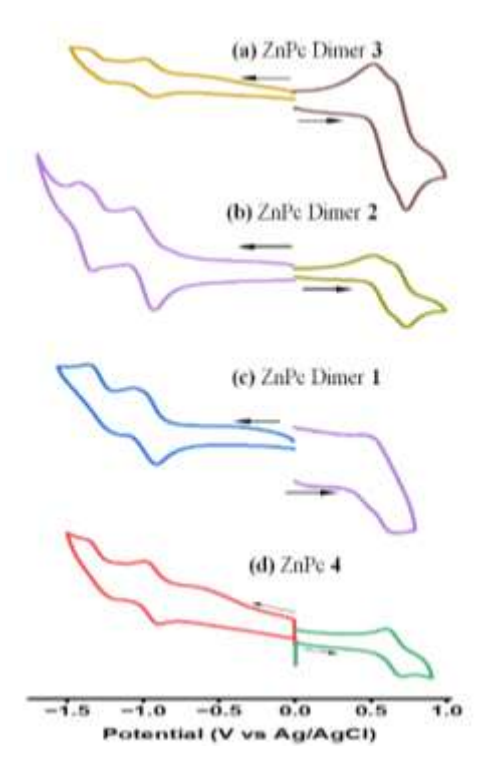


Figure 3. Cyclic voltammograms (CVs) of the indicated compounds in DCB containing 0.1 M (TBA)ClO₄ at a scan rate of 100 mV/s.

Under these conditions, the dimer's one-electron oxidized ZnPc could undergo charge resonance with the second ZnPc, as shown, thus triggering intervalence charge transfer among the two ZnPc entities. Another important observation is that of facile oxidation of the ZnPc dimers compared to the ZnPc monomer; in the case of dimers **2** and **3**, the first oxidation was easier by 80 mV compared to the monomer. This is key to observing SB-CS in the ZnPc dimer as the singlet excited energy, $E_{0,0}$ (1.76 – 1.80 V, see Table 1), would be higher than the electrochemical redox gap (1.55 to 1.56 V in DCB). This confirms that charge separation from the singlet excited state within the ZnPc dimer is thermodynamically feasible! In the above equation, K_{com} represents the comproportionality constant (see equation 5, *vide infra*).

As stated earlier, for charge resonance (intervalence charge transfer, IVCT), a new optical transition could be expected in the near-IR region, depending upon the molar absorptivity. With this in mind, spectroelectrochemical studies were performed. These studies are key to observing (i) the anticipated IVCT peak in the near-IR region. Please note that during the first electron removal, one would observe the IVCT peak; however, a second electron removal would oxidize both ZnPc entities, eliminating such optical transition. Such an observation would provide evidence of IVCT in the studied dimers. (ii) The second application of spectroelectrochemistry is to help identify charge separation products during the process of SB-CS. This is often done by performing spectroelectrochemistry during the first oxidation and reduction to generate the radical cation and radical anion spectra. Then, these two spectra are digitally added and subtracted from the neutral compound. In the event of SB-CS, the transient spectrum corresponding to the electron transfer product largely resembles this spectrum.

Figure 4 shows the spectral changes during the first oxidation and the first reduction of the investigated compounds in DCB 0.2 M (TBA)CIO₄. In the case of ZnPc monomer, **4**, the ZnPc⁻⁺

revealed two main new peaks at 528 and 844 nm while ZnPc revealed peaks a main peak at 758 nm. In contrast, for all three ZnPc dimers, a new broad peak ~1025 nm was observed that vanished during the second oxidation, providing direct proof of IVCT occurrence in the dimers. Interestingly, the radical cation peak intensity of the 844 nm was diminished. This was especially true for the strongly interacting *ortho* dimer, **3** while for the *meta* and *para* dimers, **2** and **1**, appreciable intensity for the 844 nm peak was observed in addition to the near-IR peak. During the first reduction of the ZnPc dimers, the expected peak of ZnPc was observed at 758 nm without appreciable perturbation.

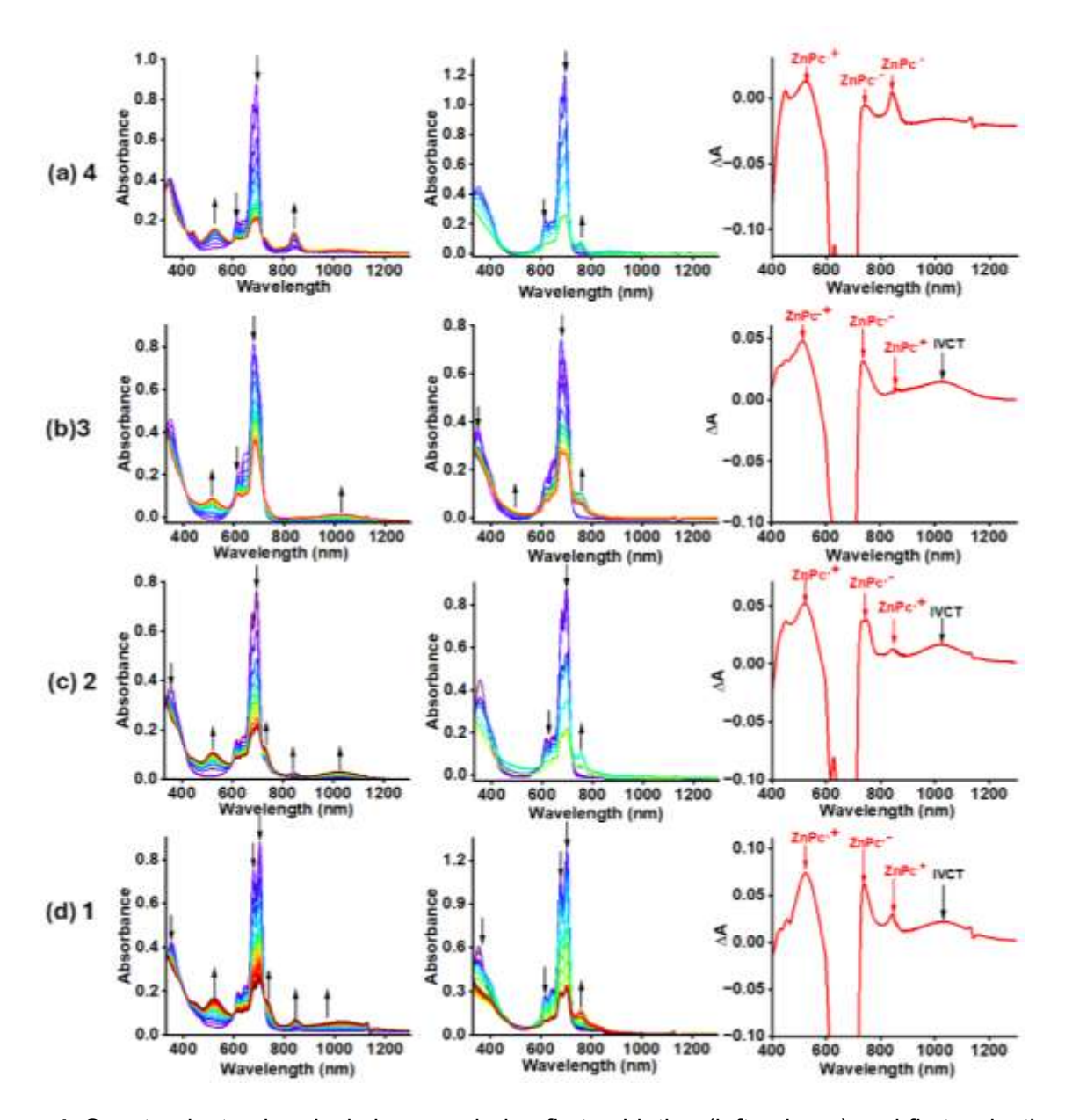


Figure 4. Spectroelectrochemical changes during first oxidation (left column) and first reduction (central column) and spectrum deduced for the charge-separated state (right column) from digital manipulation (see text for details).

The phthalocyanines could aggregate in 0.2 M supporting electrolytes, and such aggregated species could also reveal an IVCT-type transition. A close examination of the spectrochemical results of the ZnPc monomer in Figure 4a showed some absorption in the 1025 nm region. To clarify this issue, the compounds were oxidized using a chemical oxidizing agent without a supporting electrolyte, as shown in Figure S10. As expected, the absence of absorption in the 1025 nm for the ZnPc monomer was evident, while the expected IVCT peak was present for the dimers. Expectedly, the increased addition of the oxidizing agent resulted in the vanishing of the peak corresponding to the IVCT transition (expected when both ZnPc units are oxidized).

Having established IVCT in the ZnPc dimers, next, electronic coupling element, H_{IV} for the mixed-valence cation radicals of ZnPc dimers via Mulliken-Hush formalism [64,65] was performed according to equation (2).

$$H_{IV} = 0.0206 (\Delta V_{1/2} V_{max} \epsilon)^{1/2} / r_{Zn-Zn}$$
 (2)

where $\Delta v_{1/2}$ and v_{max} represent the full width at half-height and absorbance peak maxima for the charge-resonance absorption band, respectively (in cm⁻¹), ϵ is the molar extinction coefficient (in M⁻¹cm⁻¹), and r_{Zn-Zn} is the intramolecular distance between both chromophores (in Å).

Further, the position of the equilibrium could be quantitatively evaluated from the splitting according to equation (3),^[66]

$$\Delta E = -\Delta G_{com} / F \tag{3}$$

where F is the Faraday constant and $-\Delta G_{com}$ is the Gibbs free-energy change. Then, the main component of the cation-radical stabilization could be estimated according to equation (4),

$$-\Delta G_{com} = -RT \ln K_{com} \tag{4}$$

which represents electronic interaction between the redox centers. ^[63-65] The stabilization energy, ΔG_{com} , comproportionating equilibrium constant, K_{com} (eq. 5), and H_{IV} , thus calculated from the above approach, are listed in Table 2.

$$2 \operatorname{ZnPc}^{+}\operatorname{-sp-ZnPc} \stackrel{K_{\text{COM}}}{=} \operatorname{ZnPc-sp-ZnPc} + \operatorname{ZnPc}^{+}\operatorname{-sp-ZnPc}^{+} (5)$$

Table 2. Estimated electronic coupling elements for the mixed-valence cation radicals of ZnPc-dimer via Mulliken-Hush Formalism (from the IVCT band) and the associated thermodynamic parameters.

Compound	r _{Zn-Zn} a Å	<i>v_{max}</i> 10 ³ cm ⁻¹	$\Delta V_{1/2}$ $10^3 \mathrm{cm}^{-1}$	ε 10 ³ M ⁻¹ cm ⁻¹	H_{IV}^{b} 10^{3} cm^{-1}	Δ E V	- ΔG_{com} kJ/mol	K _{com}
3	13	9.57	43.48	9.4	3.16	0.14	13.5	232
2	20	9.64	48.54	6.8	1.80	0.13	12.5	155
1	23	9.57	38.76	2.0	0.77	0.12	11.6	106

^aEstimated from computational studies.

^bEstimated uncertainty is <u>+</u> 5%

Data shown in Table 2 revealed higher molar absorptivity for the IVCT band for the *ortho* dimer and subsequent higher values of $-\Delta G_{com}$, K_{com} , and H_{IV} for this dyad compared with the others. The thermodynamic feasibility for the occurrence of IVCT is also borne out from these calculations.

As mentioned earlier, another key application of spectroelectrochemical results is identifying electron transfer products during pump-probe studies. For systems revealing characteristic peaks for the radical cation and radical anion, the spectrum of these two species is digitally added and subtracted with the neutral compound. This would represent the ideal spectrum one would expect for an electron transfer product. However, care must be exercised while using such results due to the appearance of additional transient peaks (excited state absorption, ground state bleaching, stimulated emission, etc.). The spectrum corresponding to the charge-separated product for the investigated compounds is shown in Figure 4 (right column). Clear peaks of radical cation and radical anion (as marked) could be identified.

DFT and TD-DFT studies – Investigating the excited states involved in the SB-CS process

Computational studies [67-68] have become essential to probe complex photochemical events such as the SB-CS in symmetric dimers. In the event of excited state charge separation, the ground quadrupolar excited state is expected to yield bipolar (cation and anion) radical species upon photoexcitation, and such an event should be more facile in polar solvents. Figures 5, S11-13 summarize computational findings on these dimers.

As shown in Figure 5, for the optimized structures, the distance between the two ZnPc entities of the dimer was substitute-dependent on the central phenyl ring. The Zn-Zn distance in the ortho dimer was as close as 13 Å, while in meta and para dimers, they were 20 and 23 Å. In addition, the two ZnPc entities in the ortho case were almost in the interacting distance, which, for the meta dimer, the two rings were in the same plane. To evaluate the nature of excitonic interactions intrinsic to the spatial orientation of the ZnPc units, the long-range Coulombic coupling (J_{Col}) constant was computed. The dimers were fragmented into two units, and the coupling values were determined for the first bright state, the S_1 state. The (J_{Col}) values were found to be 99, 35, and 37 cm⁻¹ for the *ortho*, *meta*, and *para* dimers, respectively. A higher value for the ortho dimer suggests a strong interaction between the entities, which could be responsible for efficient charge separation as compared to the other two dimers. The frontier HOMOs and LUMOs shown in Figure S11 revealed unequal distribution among the two rings. This becomes clearer from the molecular electrostatic potential map (MEP), as shown in Figure 5. The charge localization of the quadrupolar state, $ZnPc^{\delta_{+}}$ - $sp^{\delta_{-}}$ - $ZnPc^{\delta_{-}}$, becomes better defined in benzonitrile than in the gas phase. This suggests that the ZnPc^{δ+}-sp^δ-ZnPc^{δ+} state could result in ZnPc⁺-sp-ZnPc⁻ in polar solvents upon excitation, i.e., the process of SB-CS. [33]

Figures 6 and S12, and S13 show the charge difference map (difference between the ground the excited state) and excited state MEP for the investigated dimers while the extent of orbitals involved in the different transition, their oscillator strengths, computed wavelength, change in dipole moment, and %CT versus LE are given in Tables S1-S3 for the dimers. An excited state SB-CS should result in ZnPc⁻⁺-ZnPc⁻⁻ for a given dimer and the excited states responsible for generating such charge-separated states. An unsymmetrical electron density distribution in the excited state MEP (third row) confirms the generation of ZnPc⁻⁺-ZnPc⁻⁻. As shown in Figure 6, for 3, for the first four excited states, the charge difference map and excited state MEP clearly showed charge separation (hole (blue) and electron (red)) on different ZnPc entities of the dimer. No charge separation was observed for the fifth excited state (all locally excited (LE) state). Higher oscillator strengths, the wavelength of transition falling in the near-IR region (641-688 nm), and higher %CT were observed (50-90%), and the change in dipole moment as much as 44 Debye

15213773, ja, Downloaded from https://onlinelibrary.wiley.com/doi/10.1002/anie.

was observed (Table S1). For the *meta* dimer, SB-CS was possible from the first three and fifth states (Figure S12 and Table S2). SB-CS from the first two, fourth, and 5th states was possible for the *para* dimer. The highest change in dipole moment was for the fourth transition (Figure S13 and Table S3). In summary, the TD-DFT calculations have allowed the visualization of SB-CS from different states in the present study.

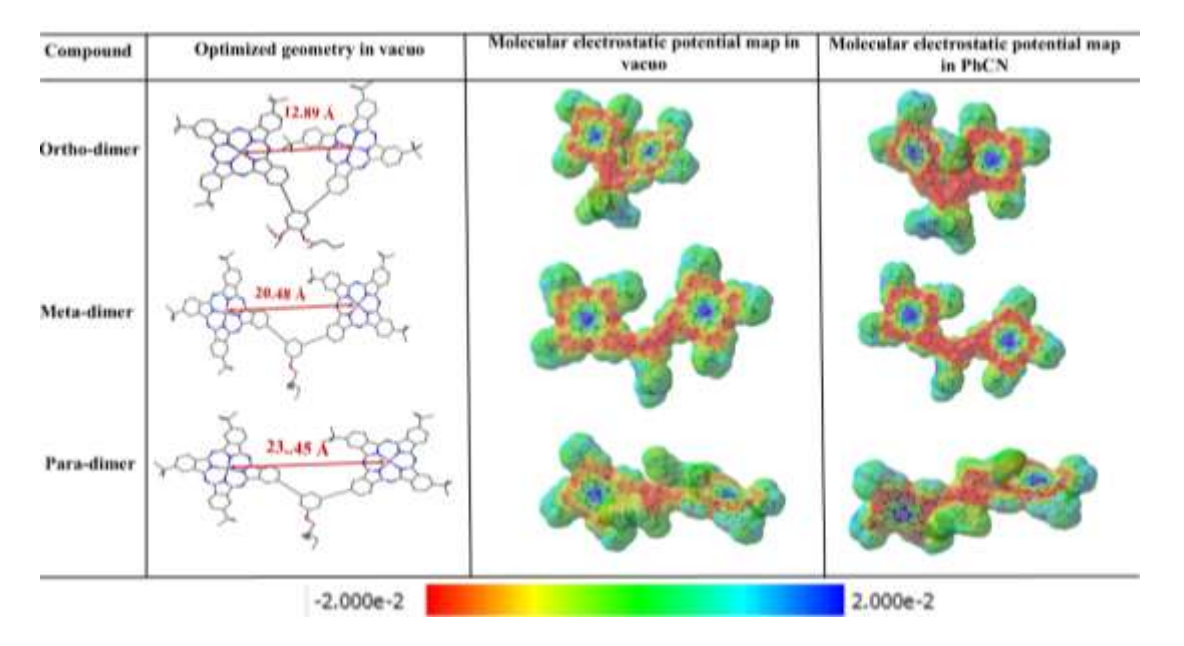


Figure 5. Gas phase optimized geometries and MEP maps in the gas (central column) and polar benzonitrile (right column), revealing the $ZnPc^{\delta_+}$ - Sp^{δ_-} - $ZnPc^{\delta_+}$ state. The dielectric continuum model (SCRF (CPCM, Solvent=Benzonitrile)) was used to probe the solvent effect.

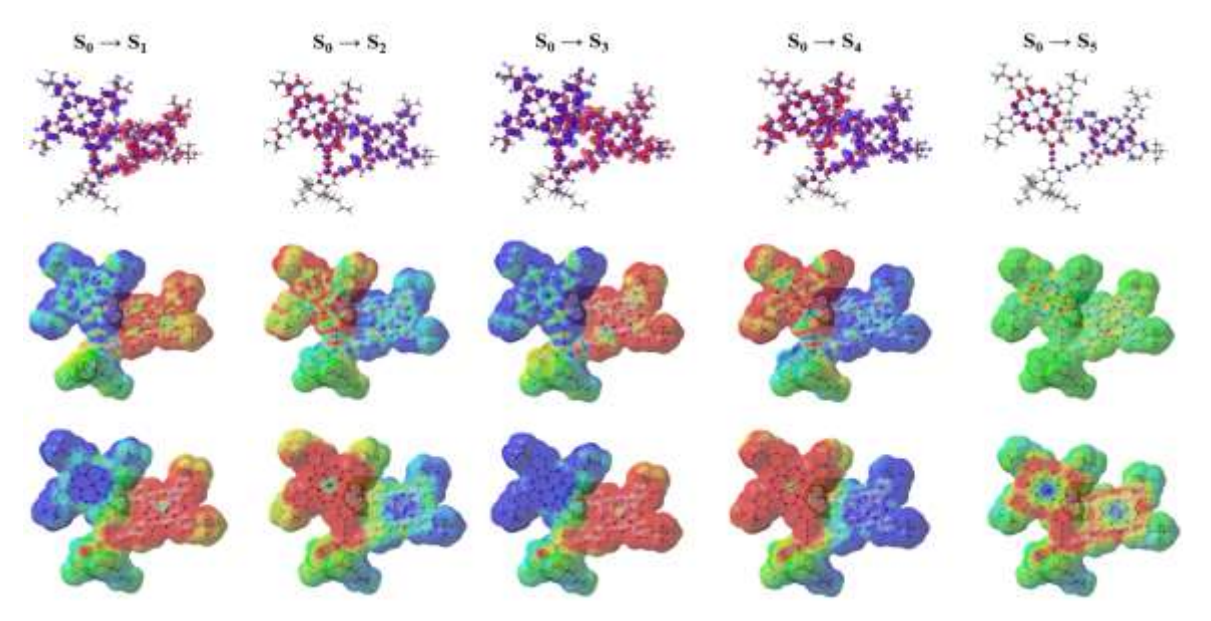


Figure 6. Distribution of hole (red) and electron (blue) for first five excited states (first row), Charge difference map (Mapped Electron Density Difference, second row, -1.00e-5 - 1.00e-5 V), and excited state MEP (third row, -2.00e-2 - 2.00e-2 V) for the dimer, **3**.

Energy diagram - Exothermic versus isoenergetic SBCS

An energy level diagram depicting different events occurring from the singlet excited state of the ZnPc dimer as a function of solvent polarity and substitution pattern is essential to visualize the SB-CS process. With this in mind, a Jablonski-type energy diagram [69] was constructed (see SI for details), as shown in Figure 7. The energy of the charge-separated states was calculated using the earlier discussed optical, electrochemical, computational, and solvation parameters From the energy diagram, it is clear that SB-CS is (dielectric continuum model). thermodynamically feasible in benzonitrile for all three dyads. Notably, the energy of the chargeseparated state is much higher than that of the ³ZnPc*. Under such conditions, the chargeseparated state could relax to the triplet state before returning to the ground state. The depicted energy diagram also shows that SB-CS is energetically harder in nonpolar toluene as the energy of the charge-separated state is higher than the pumping energy. However, it is relatively close to the ortho ZnPc dimer, 3 (40 mV difference). The earlier discussed fluorescence studies revealed efficient quenching (from both steady-state and time-resolved emission; see Figure 2c and Table 1) for this dimer, suggesting SB-CS might be possible in nonpolar toluene. If such a process could be demonstrated in toluene, this would constitute an isoenergetic (close to an endothermic) SB-CS event! Intrigued with these findings, pump-probe studies in both solvents were performed on these dimers to witness both exothermic and possible isoenergetic SB-CS processes.

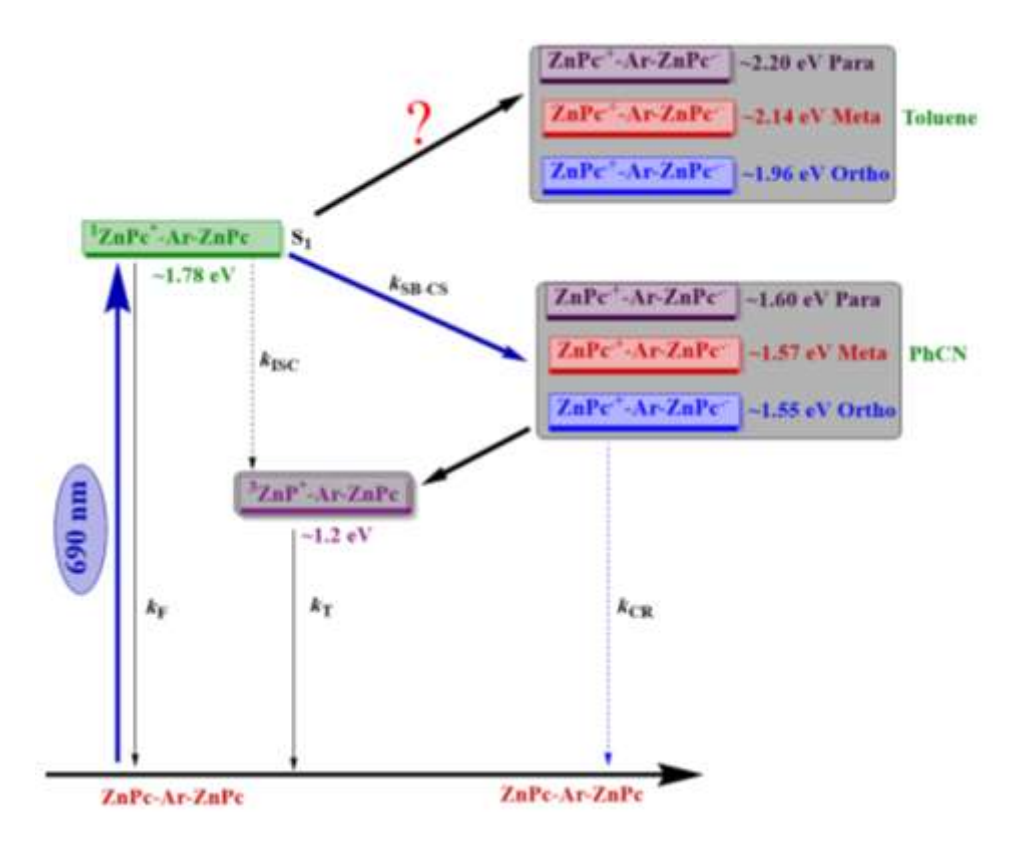


Figure 7. Jablonski-type energy level diagram showing SB-CS as a function of solvent polarity for the investigated dimers.

Femtosecond pump-probe studies – Establishing exothermic and isoenergetic SB-CS in polar and nonpolar solvents

Figure S14 shows the fs-TA spectra at the indicated delay times for the ZnPc monomer 4 in benzonitrile and toluene at the excitation wavelength of 690 nm, corresponding to the visible band. The instantaneously formed ¹ZnPc* in benzonitrile revealed excited state absorption (ESA) at 502, 590, 636, and 744 nm (see spectrum at 2.16 ps). Negative peaks at 612 and 682 nm were also observed. By comparison with the absorption and fluorescence spectra (Figure 2), the 612 nm peak was possible to assign to ground state bleaching (GSB) and the 682 nm to both GSB and stimulated emission (SE). The decay of the ESA peak and recovery of the GSB/SE peak resulted in a new transient spectra with a new peak located at 483 nm (see spectrum at 2.77 nm) that could be assigned to ³ZnPc*. The data was subjected to GloTarAn analysis ^[70-71] to generate the decay-associated spectra (DAS) and population time profiles (see Figure S14a). This analysis resulted in a lifetime of 2.1 ns for ¹ZnPc* and >3 ns for ³ZnPc*. A similar spectral trend was also observed in toluene, as shown in Figure S14b. The spectral analysis resulted in a lifetime of 2.3 ns for ¹ZnPc* and >3 ns for ³ZnPc*. The ¹ZnPc* lifetimes agreed within the experimental error from the previously obtained lifetimes from the TCSPC technique for both solvents (Table 1). In summary, for the ZnPc monomer, it was possible to establish the occurrence of $S_0 \rightarrow S_1 \rightarrow T_1 \rightarrow T_2 \rightarrow T_3 \rightarrow T_4 \rightarrow T_4 \rightarrow T_4 \rightarrow T_5 \rightarrow T_5 \rightarrow T_6 \rightarrow T_6$ GS upon photoexcitation (GS = ground state).

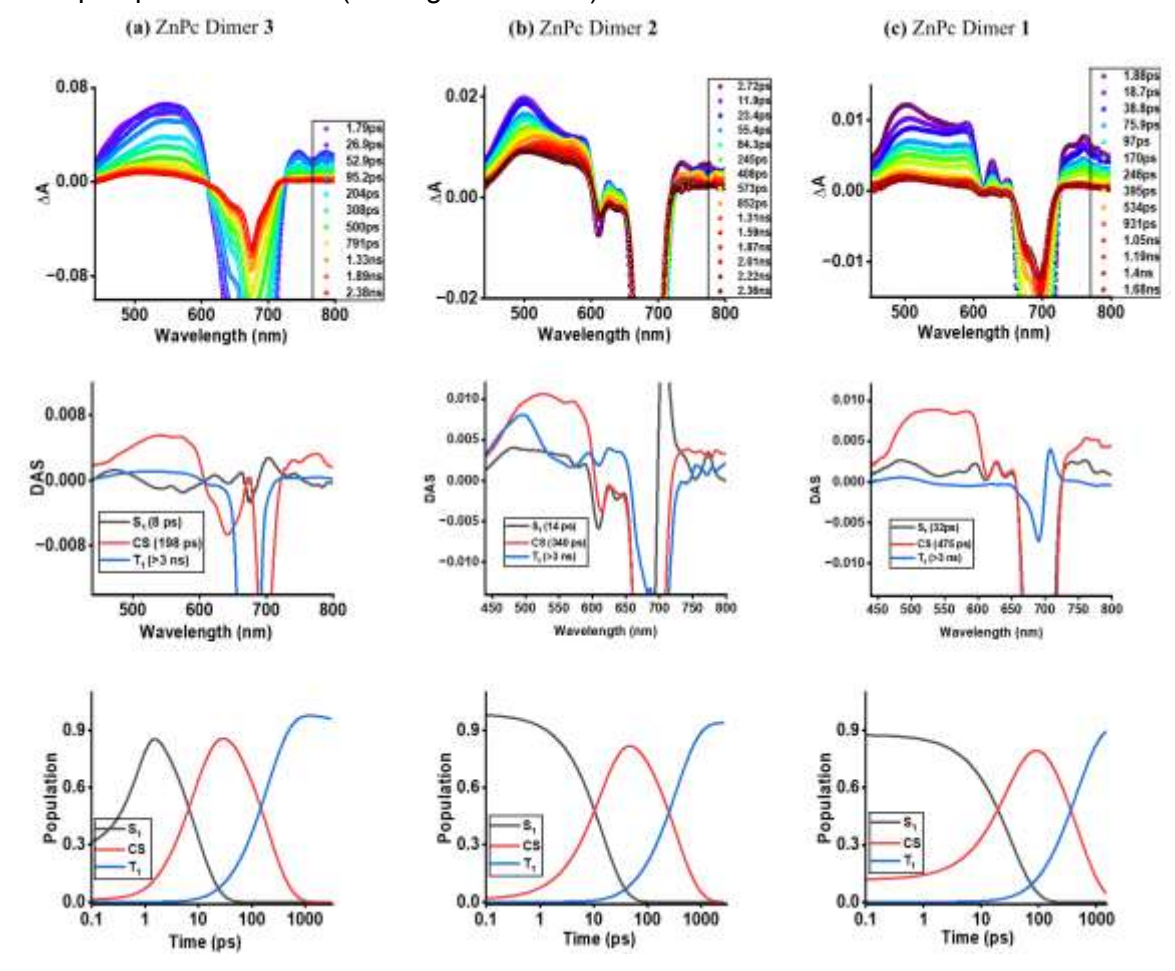


Figure 8. Fs-TA spectra at the indicated delay times for the indicated ZnPc dimers in benzonitrile, excited at 683 nm corresponding to the visible peak maxima.

The fs-TA spectra for the ZnPc dimers in benzonitrile are shown in Figure 8. In the case of all three dimers, the initially formed 1 ZnPc* evolved into a new spectrum expected for the charge-separated state (Figure 4) during the initial delay times (200-300 ps). With additional delay times, the peaks corresponding to the charge-separated state diminished in intensity, resulting in a new spectrum corresponding to the triplet state. The characteristic peak of ZnPc- $^+$ in the 520 nm range could be observed for all three dyads that were absent for the ZnP monomer (see Figure S14). These results conclusively show SB-CS in these dimers. Glotaran analysis was performed for the sequential S₁ \rightarrow CS \rightarrow T₁ events, whose DAS are shown in the middle column of Figure 8, along with the population time profiles in the bottom column. From this analysis, the average lifetime of the charge-separated state was found to be 198, 340, and 475 ps, respectively, for the *ortho, meta*, and *para* dimers. The triplet state lasted over three ns, similar to the ZnPc monomer.

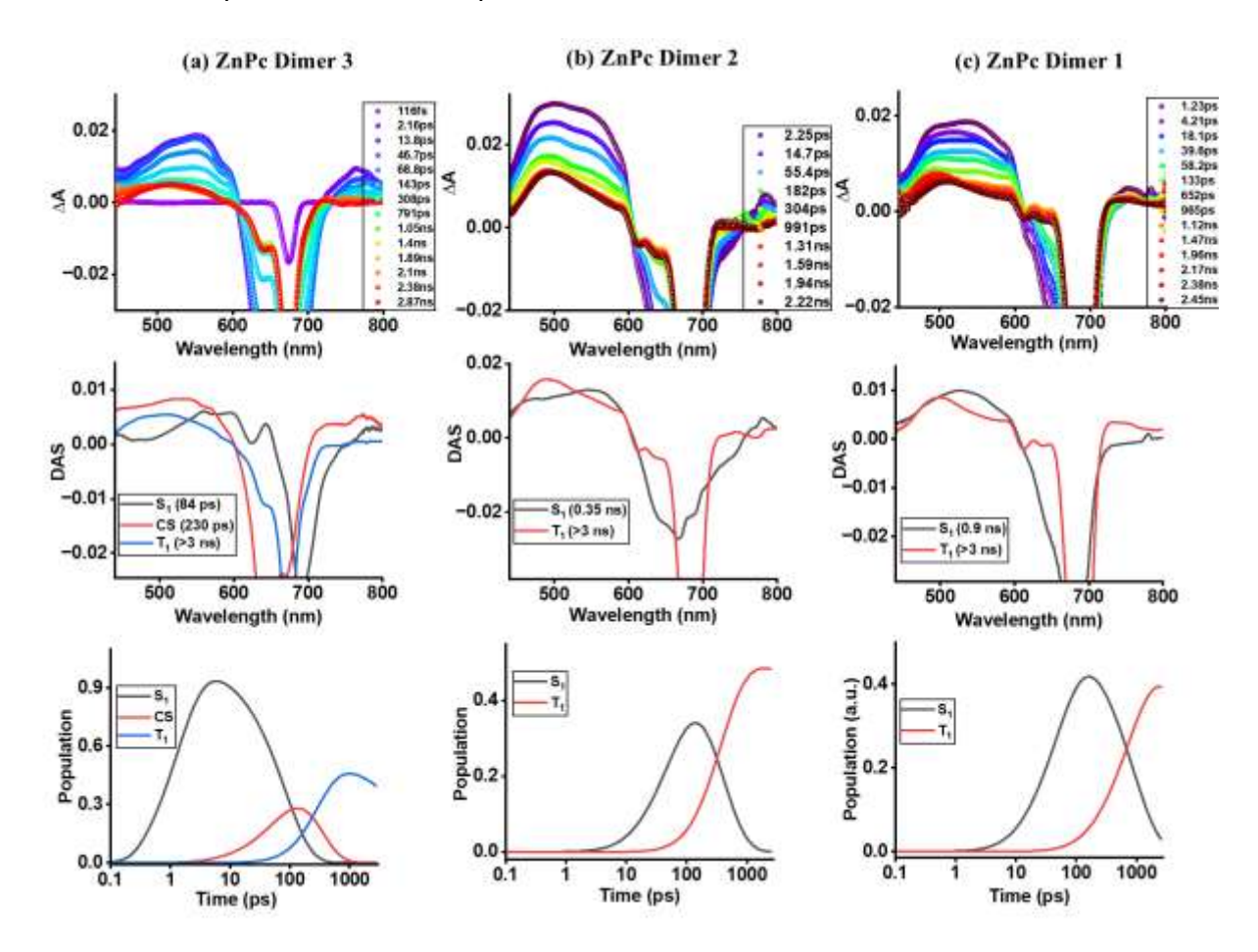


Figure 9. Fs-TA spectra at the indicated delay times for the indicated ZnPc dimers in toluene, excited at 683 nm corresponding to the visible peak maxima.

ZnPc dimers were also studied in toluene, where isoenergetic SB-CS was predicted only for the *ortho* dimer. As shown in Figure 9, this was the case where clear spectral signatures for the SB-CS were evident. However, no proof of charge separation could be obtained for the *meta* and *para* dimers. This is in accordance with the earlier discussed energy level diagram (Figure 7) where SB-CS was not expected in nonpolar toluene. In these cases, the singlet excited state populated the triplet state without the intermediacy of a charge-separated state. The DAS

revealed an average lifetime of 230 ps for the ZnPc *ortho* dimer, slightly longer than that observed in benzonitrile. Notably, the occurrence of isoenergetic SB-CS was possible to establish in the case of the *ortho* dimer in toluene. Concentration dependence studies (range = 0.1 μ M to 1.0 μ M) indicated a lack of bimolecular type electron transfer, [72] as varying concentrations did not affect the SB-CS process. If there were bimolecular electron transfer, one would expect to see increased electron transfer efficiency with an increase in dimer concentration.

Conclusion

In summary, we have successfully demonstrated intervalence charge transfer in far-red capturing ZnPc dimers for the first time. The orientation and distance of the ZnPc entities of the dimer are shown to modulate IVCT as judged by the potential difference between the split oxidation waves and the intensity of the near-IR charge transfer transition. Support for the envisioned SB-CS was initially gathered from steady-state and time-resolved fluorescence studies where quenching was observed in polar solvents. Interestingly, for the ZnPc ortho dimer, quenching occurred in both polar and nonpolar solvents. Free-energy calculations using the redox, spectral, and computational data suggested moderately endothermic (almost isoenergetic with respect to the excitation energy and energy of the charge SB-CS states) SB-CS in nonpolar toluene, making it the first example of compounds revealing SB-CS under isoenergetic conditions. The existence of a quadrupolar charge transfer state in both gas and polar media was evidenced by DFT calculations. Additionally, the conversion of the quadrupolar state to a bipolar charge-separated state, ZnPc⁻-ZnPc⁻, upon photoexcitation, was the result of TD-DFT studies. Finally, evidence of SB-CS was secured from pump-probe studies wherein peaks corresponding to the ZnPc+ and ZnPc could be identified positively. Depending upon dimer linkage, the final charge-separated states lasted 200-500 ps. The exceptional findings of both IVCT and SB-CS in ZnPc dimers of this study pave the way for their potential applications in energy harvesting and optoelectronic applications.

Acknowledgments

This work was supported by the University of North Texas, by the European Regional Development Fund "A way to make Europe" and the Spanish Ministerio de Ciencia e Innovación/Agencia Estatal de Investigación (PID2020-117855 RB-I00 to Á.S.-S) and the Generalitat Valenciana (CIPROM/2021/059 and MFA/2022/028 to Á. S.-S.). The computational work was completed at the Holland Computing Center of the University of Nebraska, which receives support from the Nebraska Research Initiative.

Keywords: Photoinduced charge separation • Intervalence charge transfer • zinc phthalocyanine • Ultrafast dynamics

- [1] G. M. Whitesides, *Angew. Chem. Int. Ed.* **2015**, *54*, 3196.
 [2] H. Satam, K. Joshi, U. Mangrolia, S. Waghoo, G. Zaidi, S
- [2] H. Satam, K. Joshi, U. Mangrolia, S. Waghoo, G. Zaidi, S. Rawool, R. P. Thakare, S. Banday, A. K. Mishra, G. Das, S. K. Malonia, *Biology* **2023**, *12*, 997.
- [3] S. V. B. P. Devaraj, S. R. Mohanty, D. J. D. Oliveira, K. T. M. A. W. M. Zhou, Wiley Interdiscip. Rev. Comput. Mol. Sci. **2024**, 14, e1725.
- [4] A. H. Proppe, Y. C. Li, A. Aspuru-Guzik, C. P. Berlinguette, C. J. Chang, R. Cogdell, A. G. Doyle, J. Flick, N. M. Gabor, R. van Grondelle, S. Hammes-Schiffer, S. A. Jaffer, S. O. Kelley, M. Leclerc,

- K. Leo, T. E. Mallouk, P. Narang, G. Schlau-Cohen, G. D. Scholes, A. Vojvodic, V. W. Yam, J. Y. Yang, E. H. Sargent, *Angew. Chem. Int. Ed.* **2020**, *59*, 828.
- [5] N. Chouhan, R.-S. Liu, Eds., *Electrochemical Technologies for Energy Storage and Conversion*, Wiley-VCH, Weinheim, **2015**.
- [6] M. R. Wasielewski, Chem. Rev. 1992, 92, 435.
- [7] D. Gust, T. A. Moore, A. L. Moore, Acc. Chem. Res. 2009, 42, 1890.
- [8] P. D. Frischmann, K. Mahata, F. Würthner, Chem. Soc. Rev. 2013, 42, 1847.
- [9] F. Würthner, T. E. Kaiser, C. R. Saha-Möller, Angew. Chem. Int. Ed. 2011, 50, 3376.
- [10] M. El-Khouly, E. El-Mohsnawy, S. Fukuzumi, *Photochemistry Reviews* **2017**, *31*, 36.
- [11] S. Fukuzumi, K. Ohkubo, F. D'Souza, J. L. Sessler, Chem. Commun. 2012, 48, 9801.
- [12] E. Romero, R. Augulis, V. I. Novoderezhkin, M. Ferretti, J. Thieme, D. Zigmantas, R. Van Grondelle, *Nat. Phys.* **2014**, *10*, 676.
- [13] M. Pessarakli, Ed. Handbook of Photosynthesis, 4th ed.; CRC Press, Boca Raton, 2024.
- [14] W. Rettig, Angew. Chem. Int. Ed Engl. 1986, 25, 971.
- [15] T. Weil, T. Vosch, J. Hofkens, K. Peneva, K. Müllen, Angew. Chem. Int. Ed. 2010, 49, 9068.
- [16] O. Ito, F. D'Souza, *Molecules* **2012**, *17*, 5835.
- [17] M. Kellogg, A. Akil, D. S. Muthiah Ravinson, L. Estergreen, S. E. Bradforth, M. E. Thompson, *Faraday Discuss.* **2019**, *216*, 379.
- [18] E. Vauthey, ChemPhysChem 2012, 13, 2001.
- [19] Y. Hou, X. Zhang, K. Chen, D. Liu, Z. Wang, Q. Liu, J. Zhao, A. Barbon, *J. Mater. Chem. C* **2019**, 7, 12048.
- [20] M. I. S. Röhr, H. Marciniak, J. Hoche, M. H. Schreck, H. Ceymann, R. Mitric, C. Lambert, J. Phys. Chem. C 2018, 122, 8082.
- [21] Y. Wu, R. M. Young, M. Frasconi, S. T. Schneebeli, P. Spenst, D. M. Gardner, K. E. Brown, F. Würthner, J. F. Stoddart, M. R. Wasielewski, *J. Am. Chem. Soc.* **2015**, *137*, 13236.
- [22] X. Wang, L. Lv, T. Li, C. Chen, X. Fan, B. Cui, L. Tang, Y. Chen, H. Liu, X. Li, *Chem. Eur. J.* **2025**, 31, e202403125.
- [23] Y. Guo, Z. Ma, X. Niu, W. Zhang, M. Tao, Q. Guo, Z. Wang, A. Xia, *J. Am. Chem. Soc.* **2019**, *141*, 12789.
- [24] J. Kong, W. Zhang, G. Li, D. Huo, Y. Guo, X. Niu, Y. Wan, B. Tang, A. Xia, *J. Phys. Chem. Lett.* **2020**, *11*, 10329.
- [25] S. Parida, S. K. Patra, S. Mishra, *J. Phys. Chem. B* **2024**, *128*, 9873.
- [26] A. Mazumder, K. Vinod, P. D. Maret, P. P. Das, M. Hariharan, J. Phys. Chem. Lett. 2024, 15, 5896.
- [27] F. C. Spano, J. Phys. Chem. C 2024, 128, 248.
- [28] X. Chang, B. M. Qarai, F. C. Spano, *Chem. Mater.* **2023**, 35, 10018.
- [29] P. D. Maret, D. Sasikumar, E. Sebastian, M. Hariharan, J. Phys. Chem. Lett. 2023, 14, 8667.
- [30] B. S. Basel, J. Zirzlmeier, C. Hetzer, S. R. Reddy, B. T. Phelan, M. D. Krzyaniak, M. K. Vollard, P. D. Coto, R. M. Young, T. Clark, M. Thoss, R. R. Tykwinski, M. R. Wasielewski, D. M. Guldi, *Chem* **2018**, *4*, 1092.
- [31] V. Markovic, D. Villamaina, I. Barabanov, L. M. Lawson Daku, E. Vauthey, *Angew. Chem. Int. Ed.* **2011**, *50*, 7596.
- [32] J. H. Golden, L. Estergreen, T. Porter, A. C. Tadle, M. R. D. Sylvinson, J. W. Facendola, C. P. Kubiak, S. E. Bradforth, M. E. Thompson, *ACS Appl. Energy Mater.* **2018**, *1*, 1083.
- [33] A. Yahagh, R. R. Kaswan, S. Kazemi, P. A. Karr, F. D'Souza, Chem. Sci. 2024, 15, 906.
- [34] C. Trinh, K. Kirlikovali, S. Das, M. E. Ener, H. B. Gray, P. Djurovich, S. E. Bradforth, M. E. Thompson, *J. Phys. Chem. C* **2014**, *118*, 21834.
- [35] J. J. Piet, W. Schuddeboom, B. R. Wegewijs, F. C. Grozema, J. M. Warman, *J. Am. Chem. Soc.* **2001**, *123*, 5337.
- [36] P. Roy, G. Bressan, J. Gretton, A. N. Cammidge, S. R. Meech, *Angew. Chem. Int. Ed.* **2021**, *60*, 10568.
- [37] X. Zhao, J. P. O'Connor, J. D. Schultz, Y. J. Bae, C. Lin, R. M. Young, M. R. Wasielewski, *J. Phys. Chem. B* **2021**, *125*, 6945.
- [38] N. Powers-Riggs, X. Zuo, R. M. Young, M. R. Wasielewski, *J. Am. Chem. Soc.* **2019**, *141*, 17512.

- [39] C. E. Ramirez, S. Chen, N. Powers-Riggs, I. Schlesinger, R. M. Young, M. R. Wasielewski, *J. Am. Chem. Soc.* **2020**. *142*. 18243.
- [40] A. Khan, N. A. Tcyrulnikov, R. Roy, R. M. Young, M. R. Wasielewski, A. L. Koner, J. Phys. Chem. C 2024, 128, 10474.
- [41] S. S. Rajasree, H. C. Fry, D. J. Gosztola, B. Saha, R. Krishnan, P. Deria, *J. Am. Chem. Soc.* **2024**, 146, 5543.
- [42] S. Kang, W. Choi, J. Ahn, T. Kim, J. H. Oh, D. Kim, ACS Appl. Mater. Interfaces 2024, 16, 18134.
- [43] N. J. Hestand, F. C. Spano, Chem. Rev. 2018, 118, 7069.
- [44] D. W. Lawlor, *Photosynthesis*, 3rd ed.; Elsevier: Amsterdam, **1987**.
- [45] J. Deisenhofer, J. R. Norris, *Photosynthetic Reaction Center*, Vol. 2; Academic Press, **2013**.
- [46] C. N. Hunter, F. Daldal, M. C. Thurnauer, J. T. Beatty, The Purple Phototrophic Bacteria, 2009.
- [47] M. T. Madigan, D. O. Jung, An overview of purple bacteria: systematics, physiology, and habitats. The Purple Phototrophic Bacteria; Advances in photosynthesis and respiration; Springer: Dordrecht. **2009**. Vol. 28.
- [48] J. Hankache, O. S. Wenger, *Chem. Rev.* **2011**, *111*, 5138.
- [49] A. Heckmann, C. Lambert, *Angew. Chem. Int. Ed.* **2012**, *51*, 326.
- [50] I. C. Lewis, L. S. Singer, J. Chem. Phys. 1965, 43, 2712.
- [51] D. B. Brown, *Mixed-valence compounds; theory and applications in chemistry, physics, geology, and biology.* New York, NY: Reidel, **1980**.
- [52] S. F. Nelsen, R. F. Ismagilov, D. A. Trieber, *Science* **1997**, 278, 846.
- [53] A. Aviram, M. A. Ratner, Chem. Phys. Lett. 1974, 29, 277.
- [54] H. Song, M. A. Reed, T. Lee, Adv. Mater. 2011, 23, 1583.
- [55] G. C. Solomon, D. Q. Andrews, R. P. V. Duyne, M. A. Ratner, J. Am. Chem. Soc. 2008, 130, 7788.
- [56] C. Creutz, H. Taube, J. Am. Chem. Soc. 1969, 91, 3988.
- [57] C. Creutz, H. Taube, *J. Am. Chem. Soc.* **1973**, 95, 1086.
- [58] M. B. Robin, P. Day, *Mixed Valence Chemistry: A Survey and Classification*. In: Emeleus, H.J. and Sharpe, A.G., Eds., *Advances in Inorganic Chemistry and Radiochemistry*, Vol. 10, Academic Press, New York, **1967**, 247.
- [59] a) G. de la Torre, G. Bottari, T. Torres, Adv. Energy Mater. 2017, 7, 1601700; b) T. Furuyama, K. Satoh, T. Kushiya, N. Kobayashi, J. Am. Chem. Soc. 2014, 136, 765; c) N. Kobayashi, T. Furuyama, K. Satoh, J. Am. Chem. Soc. 2011, 133, 19642.
- [60] A. L. Thomas, Phthalocyanine Research and Applications; CRC Press, 1990.
- [61] A. B. Sorokin, Chem. Rev. 2013, 113, 8152.
- [62] F. D'Souza, O. Ito, Chem. Commun. 2009, 4913.
- [63] N. S. Hush, R. J. Hobbs, Prog. Inorg. Chem. 1967, 8, 391.
- [64] M. Rust, J. Lappe, R. J. Cave, J. Phys. Chem. A 2002, 106, 3930.
- [65] S. Amthor, C. Lambert, J. Phys. Chem. 2006, 110, 1177.
- [66] D.-L Sun, S. V. Rosokha, S. V. Lindeman, J. K. Kochi, J. Am. Chem. Soc. 2003, 125, 15950.
- [67] Gaussian 16, Revision A.03, M. J. Frisch, G. W. Trucks, H. B. Schlegel, G. E. Scuseria, M. A. Robb, J. R. Cheeseman, G. Scalmani, V. Barone, B. Mennucci, G. A. Petersson, H. Nakatsuji, M. Caricato, X. Li, H. P. Hratchian, A. F. Izmaylov, J. Bloino, G. Zheng, J. L. Sonnenberg, M. Hada, M. Ehara, K. Toyota, R. Fukuda, J. Hasegawa, M. Ishida, T. Nakajima, Y. Honda, O. Kitao, H. Nakai, T. Vreven, J. A. Montgomery Jr., J. E. Peralta, F. Ogliaro, M. Bearpark, J. J. Heyd, E. Brothers, K. N. Kudin, V. N. Staroverov, R. Kobayashi, J. Normand, K. Raghavachari, A. Rendell, J. C. Burant, S. S. Iyengar, J. Tomasi, M. Cossi, N. Rega, J. M. Millam, M. Klene, J. E. Knox, J. B. Cross, V. Bakken, C. Adamo, J. Jaramillo, R. Gomperts, R. E. Stratmann, O. Yazyev, A. J. Austin, R. Cammi, C. Pomelli, J. W. Ochterski, R. L. Martin, K. Morokuma, V. G. Zakrzewski, G. A. Voth, P. Salvador, J. J. Dannenberg, S. Dapprich, A. D. Daniels, Ö. Farkas, J. B. Foresman, J. V. Ortiz, J. Cioslowski, D. J. Fox, Gaussian, Inc., Wallingford CT, USA, 2016.
- [68] R. Dennington, T. A. Keith, J. M. Millam, *GaussView 6.0.*16, Semichem Inc., Shawnee Mission, 2016.
- [69] D. Rehm, A. Weller, *Israel J. Chem.* **1970**, *8*, 259.
- [70] J. J. Snellenburg, S. Laptenok, R. Seger, K. M. Mullen, I. H. M. van Stokkum, *J. Stat. Softw.* **2012**, 49, 1.

- http://glotaran.org/
- [71] [72] H. Liu, Z. Li, X. Zhang, Y. Xu, G. Tang, Z. Wang, Y.-Y. Zhao, M-R. Ke, B-Y Zheng, S. Huang, J.-D. Huang, X. Li. *Nature Commun.* **2025**, *16*, 326 (1-15).

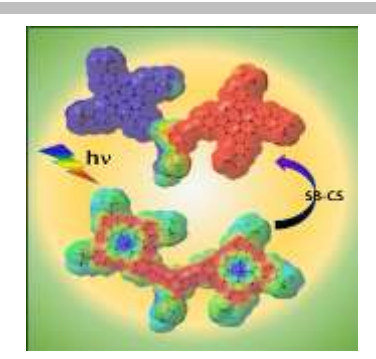
Entry for the Table of Contents

Isoenergetic-symmetry-breaking charge separation

R. R. Kaswan, D. Molina, L. Ferrer-López, J. Ortiz, P. A. Karr, Á. Sastre-Santos, * F. D'Souza*

Page No. - Page No.

Intervalence Charge Transfer and Exothermic and Isoenergetic Symmetry Breaking Charge Separation in Far-Red Capturing Zinc Phthalocyanine Dimers



The occurrence of intervalence charge transfer and exothermic and isoenergetic symmetry-breaking charge separation in far-red capturing zinc phthalocyanine dimers is demonstrated. Further, the splitting of redox peak and near-infrared IVCT signal have been used as diagnostic markers to prove the IVCT mechanism and occurrence of SB-CS in newly synthesized identical pairs of ZnPc chromophores.